JACS
JOURNAL OF THE AMERICAN CHEMICAL SOCIETY
Article
pubs.acs.org/JACS

A Robust and Versatile Photoinduced Living Polymerization of Conjugated and Unconjugated Monomers and Its Oxygen Tolerance

Jiangtao Xu,[†,‡] Kenward Jung,[†] Amir Atme,[‡] Sivaprakash Shanmugam,[†] and Cyrille Boyer*[,†,‡]

[†]Centre for Advanced Macromolecular Design (CAMD), School of Chemical Engineering, and [‡]Australian Centre for NanoMedicine, School of Chemical Engineering, UNSW Australia, Sydney, NSW 2052, Australia

Supporting Information

ABSTRACT: Controlled/living radical polymerization techniques have transformed polymer chemistry in the last few decades, affording the production of polymers with precise control over both molecular weights and architectures. It is now possible to synthesize almost an infinite variety of macromolecules using nonspecialized equipment, finding applications in high-tech industry. However, they have several shortcomings. Until recently, living radical polymerizations could not be controlled by an external stimulus, such as visible light, pH, mechanical, chemical, etc. Moreover, they are usually sensitive to trace amounts of oxygen in the system. In this Article, we report a photoinduced living polymerization technique, which is able to polymerize a large range of monomers, including conjugated and unconjugated monomers, using ultralow concentrations of an iridium-based photoredox catalyst (typically 1 ppm to monomers) and a low energy visible LED as the light source (1−4.8 W, λ_{max} = 435 nm). The synthesis of homopolymers with molecular weights ranging from 1000 to 2 000 000 g/mol was successfully achieved with narrow molecular weight distributions (M_w/M_n < 1.3). In addition, chain extensions of poly(methacrylate)s, poly(styrene), poly(*N*-vinyl pyrrolidinone), poly(vinyl ester)s, and poly(acrylate)s were performed to prepare diblock copolymers. The reusability of the catalyst was demonstrated by the synthesis of a decablock polymer by multiple chain extensions. Most importantly, this process was employed to prepare well-defined polymers and multiblock copolymers in the presence of air.

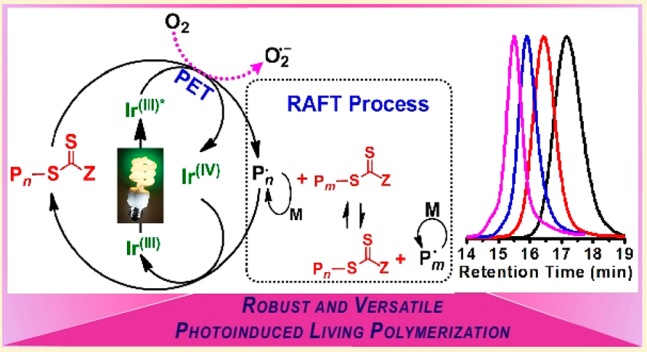

INTRODUCTION

The development of controlled polymerization techniques triggerable by stimulus, including photochemical, thermal, and electrochemical stimuli, has grown in interest due to their unique abilities to be switched between "ON" and "OFF" states.[1−16] Since the seminal work of Otsu and co-workers,[17] radical polymerization triggered by light has attracted a great deal of attention due to the ease in control of polymerizations in both space and time.[10,18−20] It has been demonstrated that this technique can be used to prepare various architectures, such as block, graft, and star polymers. Recently, with the emergence of reversible addition−fragmentation chain transfer (RAFT) polymerization,[21−24] thiocarbonylthio compounds were successfully employed for photocontrolled radical polymerization in the presence or absence of photoinitiators.[10,18,19,25,26] Despite some success in employing these techniques, they were not without limitations, most notably, the loss of end-group fidelity due to the photolysis of the RAFT end-group under UV light.[27−29]

Inspired by the early works of Stephenson,[30−34] Yoon,[35,36] and Macmillan[37,38] on the atom transfer radical addition (ATRA) of halide compounds onto olefins catalyzed by a photoredox catalyst and by the recent works of Lalevée on free radical polymerization using photocatalysts, Hawker and co-workers[3] developed an analogue of atom transfer radical polymerization (ATRP) controllable by light in 2012. A versatile photocontrolled polymerization technique able to polymerize a broader range of monomers, including both conjugated monomers ((meth)acrylate, (meth)acrylamide, and styrene) and unconjugated monomers (vinyl esters, *N*-vinyl pyrrolidinone, and dimethyl vinylphosphonate), preferably under low energy visible light (low wattage), would be desirable.

We envisioned a new photoinduced living polymerization technique that would be able to polymerize a large range of monomers, even in the presence of oxygen. In this technique, a photoredox catalyst (in our case, *fac*-[Ir(ppy)$_3$], $Ir^{(III)}$, Supporting Information, Scheme S1) was employed to generate an excited species ($Ir^{(III)}$*) under irradiation, which was then able to reduce thiocarbonylthio compounds via photoinduced electron transfer (PET),[37] resulting in the production of radicals ($P_n^{\bullet}$) and $Ir^{(IV)}$ species (Scheme 1). In contrast to the conventional RAFT mechanism, the thiocarbonylthio compound in this technique acted as an initiator in addition to being a chain transfer agent. The radical ($P^{\bullet}$), generated by the

Received: February 18, 2014
Published: April 1, 2014

   dx.doi.org/10.1021/ja501745g | *J. Am. Chem. Soc.* 2014, 136, 5508−5519

Scheme 1. Proposed Mechanism of a Photoinduced Living Polymerization Using *fac*-[Ir(ppy)$_3$] as Photoredox Catalyst

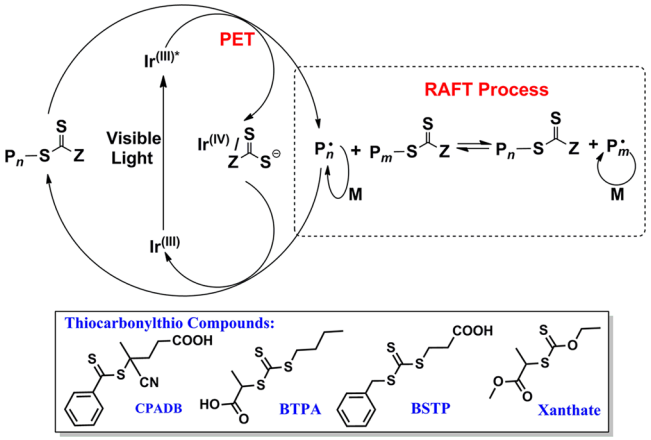

reduction of thiocarbonylthio compound via PET process, could initiate polymerization of the monomers. The radical (P$^{\bullet}$) may then participate in the RAFT process or be deactivated by Ir$^{(IV)}$ to regenerate the initial Ir$^{(III)}$, which would restart the catalytic cycle. Thus, this process involves an electron transfer process between the photocatalyst and the thiocarbonylthio compound and a cooperative RAFT process. This technique presents several further merits in comparison to the conventional RAFT mechanism. The polymerization reactions can be performed at room temperature using low energy blue light (1−4.8 W, λ_{max} = 435 nm) in tandem with catalyst doses in the ppm range. More importantly, the elimination of exogenous radical initiators limits the formation of dead polymers. We employed this photoinduced living polymerization technique for the controlled polymerization of a range of different monomers, including methacrylates, acrylates, styrene, acrylamides, methacrylamides, vinyl esters, vinyl phosphonate, and *N*-vinyl pyrrolidinone monomers (Scheme 2). The synthesis of multiblock polymers via successive chain extensions was also achieved to yield complex block polymers. Finally, we exploited the strong reductive properties of *fac*-[Ir(ppy)$_3$] to activate the polymerization without prior deoxygenation processes, which resulted in the synthesis of well-defined polymers with narrow molecular weight distributions.

RESULTS AND DISCUSSION

1. Investigation of Photoinduced Living Polymerization Mechanism Using Fluorescence Spectroscopy and Cyclic Voltammetry. The proposed mechanism for photoinduced living polymerization described in Scheme 1 is based on a photoredox reaction between a thiocarbonylthio compound and a photoredox catalyst. The redox potential of Ir$^{(IV)}$/Ir$^{(III)}$* is −1.72 V (potential versus the saturated calomel electrode (SCE) in acetonitrile),[34,39] whereas the redox potentials of thiocarbonylthio compounds are usually higher,[40,41] −0.4, −0.6, and −0.9 V (potential versus SCE) for CPADB, BTPA, and BSTP, respectively (Supporting Information, Figure S2). As the redox potentials are all greater than −1.72 V, we expected that Ir$^{(III)}$* will be able to reduce the thiocarbonylthio compounds via the photoelectron transfer (PET) process. To prove the electron transfer between *fac*-[Ir(ppy)$_3$] and the thiocarbonylthio compound did occur, fluorescence quenching (or Stern−Volmer quenching) studies

Scheme 2. [a]

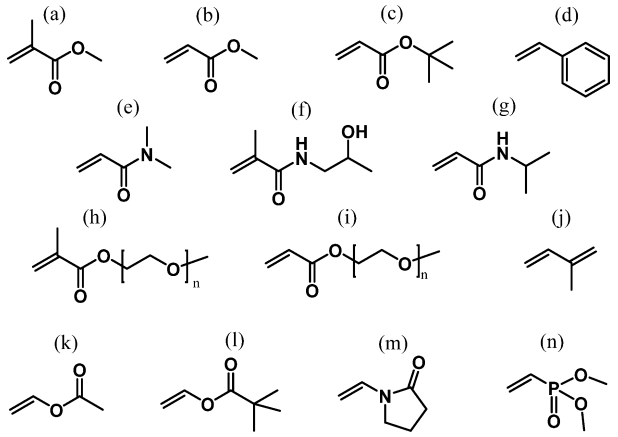

[a]List of monomers investigated in this study: (a) methyl methacrylate (MMA), (b) methyl acrylate (MA), (c) *tert*-butyl acrylate (*t*BuA), (d) styrene (St), (e) *N*,*N*-dimethylacrylamide (DMA), (f) *N*-(2-hydroxypropyl) methacrylamide (HPMA), (g) *N*-isopropylacrylamide (NIPAAm), (h) oligoethylene glycol methyl ether methacrylate (OEGMA), (i) oligoethylene glycol methyl ether acrylate (OEGA), (j) isoprene, (k) vinyl acetate, (l) vinyl pivalate (VP), (m) *N*-vinyl pyrolidinone (NVP), (n) dimethyl vinylphosphonate (DVP).

were performed. *fac*-[Ir(ppy)$_3$] catalyst (Ir$^{(III)}$) is a fluorescent compound, with an excitation and emission wavelength at 376 and 524 nm, respectively, in DMSO (Supporting Information, Figure S3). In these quenching experiments, the concentration of the thiocarbonylthio compound in a solution of *fac*-[Ir(ppy)$_3$] was gradually increased, and the intensity of the fluorescence emission peak at 524 nm was measured. We observed a decrease in the emission intensity (I) after addition of the thiocarbonylthio compound (Figure 1A), which confirmed energy transfer between *fac*-[Ir(ppy)$_3$] and the thiocarbonylthio compound. Plotting the ratio I_0/I versus the quencher concentration showed a nonlinear relationship, indicative of both dynamic and static quenching behaviors. In the case of dynamic quenching (also called collisional quenching), the excited state of *fac*-[Ir(ppy)$_3$] transfers the energy to the thiocarbonylthio compound, whereas static quenching results in the formation of a complex (Figure 1B).

2. Polymerization of Methyl Methacrylate by Photoinduced Living Polymerization. After proving that energy transfer occurred between the thiocarbonylthio compounds and excited Ir$^{(III)}$*, we decided to test our process for the polymerization of methyl methacrylate (MMA) using a dithiobenzoate (CPADB, Scheme 1) as initiator and chain transfer agent, *fac*-[Ir(ppy)$_3$] as catalyst, and a 4.8 W blue LED light source in *N*,*N*′-dimethylformamide (DMF) (Table 1, no. 1). Poly(methyl methacrylate) (PMMA) polymers were obtained with relatively good control of the molecular weights and narrow molecular weight distributions (MWDs). These results motivated us to reduce the concentration of catalyst to 1 ppm (Table 1, no. 2). After 67 h, 73% monomer conversion was determined by nuclear magnetic resonance (NMR), demonstrating that the successful polymerization could be performed at very low concentrations of catalyst. Although decreasing the catalyst concentration also resulted in slightly slower polymerization kinetics, such ultralow concentration of catalyst is potentially desirable for industrial applications.

Inspired by the initial work of Stephenson and co-workers[34] on the efficiency of the catalyst for organic reactions, we

dx.doi.org/10.1021/ja501745g | J. Am. Chem. Soc. 2014, 136, 5508−5519

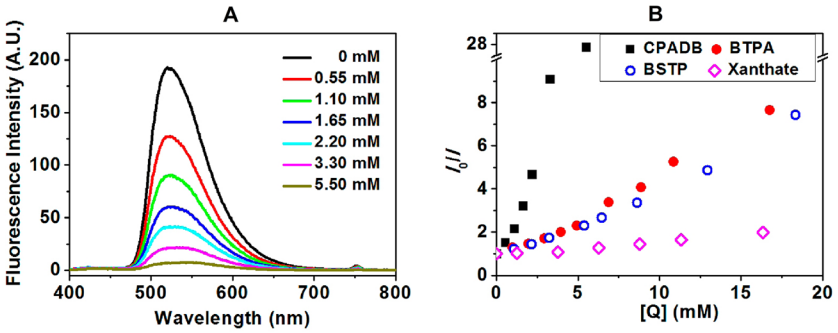

Figure 1. Fluorescence quenching studies of a 7.64 μM solution of *fac*-[Ir(ppy)$_3$] in DMSO with varying concentrations of thiocarbonylthio compounds (CPADB, BTPA, BSTP, and xanthate). (A) Fluorescent emission intensity versus different concentrations of CPADB; (B) plots of the ratio I_o/I versus quencher concentration. I_o and I correspond to the emission intensity in the absence and presence of quencher, respectively.

Table 1. Examples of PMMA Synthesized in This Study

no.	exp. cond.[a] [M]:[CPADB]:[Ir]	solvent	[Ir]/[M] (ppm)	time (h)	α[b] (%)	$M_{n,th}$[c] (g/mol)	$M_{n,GPC}$[d] (g/mol)	M_w/M_n[d]
1	200:1:10 × 10^{-4}	DMF	5	23	69	14 120	14 300	1.18
2	200:1:2 × 10^{-4}	DMF	1	67	73	14 520	14 700 (15 100)[e]	1.09
3	200:1:4 × 10^{-4}	DMSO	2	24	71	14 620	14 100	1.12
4	200:1:2 × 10^{-4}	DMSO	1	36	85	17 260	17 000	1.09
5	4000:1:40 × 10^{-4}	DMSO	1	24	88	352 200	335 000	1.23
6	200:1:0	DMSO	0	48	0	0		

[a]The reactions were performed at room temperature under 4.8 W blue LED light (λ_{max} = 435 nm). [b]Monomer conversion determined by ^{1}H NMR spectroscopy was calculated by the following equation: $\alpha = (1 - [(I^{5.5-6.0ppm}/2)/(I^{3.5ppm}/3)]) \times 100$. [c]Theoretical molecular weight calculated using the following equation: $M_{n,th} = [MMA]_0/[CPADB]_0 \times MW^{MMA} \times \alpha + MW^{CPADB}$, where $[MMA]_0$, $[CPADB]_0$, MW^{MMA}, α, and MW^{CPADB} correspond to MMA and CPADB concentration, molar mass of MMA, monomer conversion, and molar mass of CPADB. [d]Molecular weight and polydispersity determined by GPC analysis (DMAc used as eluent). [e]Molecular weight determined by ^{1}H NMR using $M_{n,NMR} = (I^{3.5ppm}/3)/(I^{7.2-7.8ppm}/5) \times MW^{MMA} + MW^{CPADB}$, where $I^{3.5ppm}$ and $I^{7.2-7.8ppm}$ correspond to integrals of signal at δ 3.5 ppm and δ 7.2−7.8 ppm attributed to OCH_3 of MMA and phenyl group of CPADB, respectively.

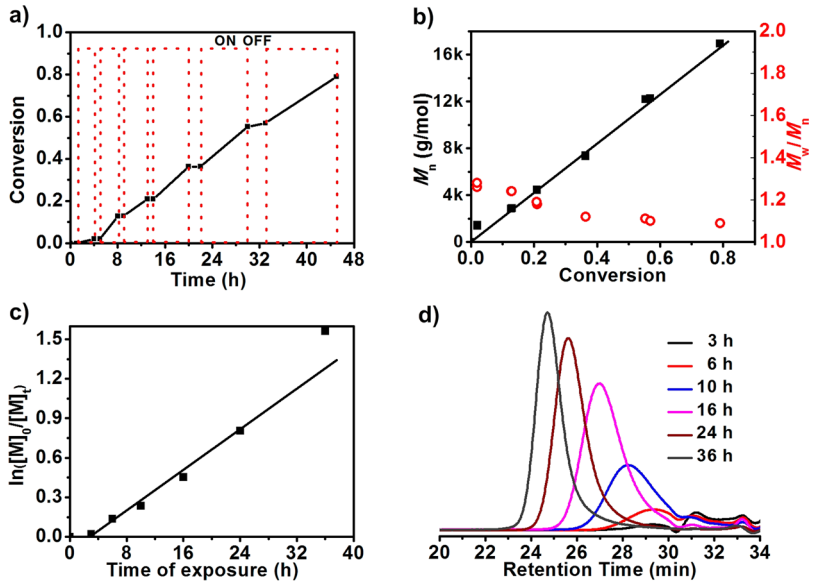

Figure 2. Photopolymerization of MMA using CPADB and *fac*-[Ir(ppy)$_3$] as photoredox catalyst in the presence ("ON") or in the absence ("OFF") of light: (a) conversion versus time; (b) $\ln([M]_0/[M]_t)$ versus time of exposure; (c) M_n (●) and M_w/M_n (○) versus conversion; and (d) GPC traces at different times of exposure. Room temperature; 4.8 W blue LED light; [MMA]:[CPADB]:[catalyst] = 200:1:10 × 10^{-4}.

initiated the exploration of other solvents, including dimethyl sulfoxide (DMSO), acetonitrile, toluene, and methanol (Supporting Information, Tables S1 and S2). Successful polymerizations were obtained for all of these solvents, which demonstrated the versatility of this polymerization technique. Consistent with previous observations in organic and polymer synthesis,[6,8,32,42] we observed that DMSO allowed for significantly faster polymerization kinetics and lower M_w/M_n values, suggesting higher catalytic efficiency as compared to other solvents (Table 1, nos. 3−5). Different M_n's of PMMA were prepared in DMSO ranging from 2500 to 350 000 g/mol with narrow MWDs, M_w/M_n < 1.30, validating the versatility of

dx.doi.org/10.1021/ja501745g | J. Am. Chem. Soc. 2014, 136, 5508−5519

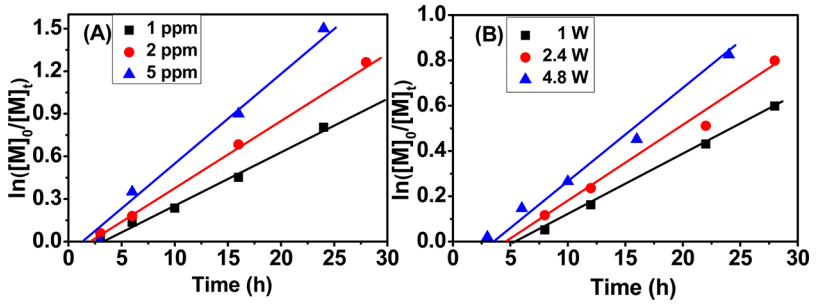

Figure 3. Photopolymerization of MMA using (A) varied concentrations of photoredox catalyst and (B) different light intensities of blue LED (λ_{max} = 435 nm) in the presence of CPADB at room temperature, using a molar ratio of [MMA]:[CPADB] = 200:1 in DMSO.

Table 2. Examples of Polymers Synthesized Using Conjugated Monomers in This Study

no.	exp. cond.[a] [M]:[thiocar]:[Ir]	monomer	thiocar	[Ir]/[M] (ppm)	time (h)	α[b] (%)	$M_{n,th}$[c] (g/mol)	$M_{n,GPC}$[d] (g/mol)	M_w/M_n[d]
1	$200:1:10 \times 10^{-4}$	HPMA	CPADB	5	24	70	20 300	58 600 (24 210)[e]	1.16
2	$400:1:20 \times 10^{-4}$	HPMA	CPADB	5	24	72	41 000	49 200	1.08
3	$200:1:2 \times 10^{-4}$	HPMA	CPADB	1	24	21	6280	12 100 (6490)[e]	1.09
4	$200:1:10 \times 10^{-4}$	MA	BTPA	5	2	99	17 800	17 500	1.05
5	$200:1:2 \times 10^{-4}$	MA	BTPA	1	2	93	16 170	15 500	1.08
6	$200:1:4 \times 10^{-5}$	MA	BTPA	0.2	10	96	16 770	17 100	1.12
7	$200:1:2 \times 10^{-5}$	MA	BTPA	0.1	10	83	14 530	15 300	1.19
8	$200:1:2 \times 10^{-4}$	MA	BSTP	1	2	88	14 640	15 430	1.13
9	$40:1:2 \times 10^{-4}$	OEGA	BTPA	5	8	81	14 630	15 800	1.11
10	$200:1:10 \times 10^{-4}$	*t*BA	BTPA	5	2	88	25 480	22 200	1.09
11	$200:1:20 \times 10^{-4}$	St	BTPA	10	48	50	9630	9100	1.13
12	$200:1:20 \times 10^{-3}$	St	BTPA	100	24	89[f]	18 810[f]	18 700[f]	1.21[f]
13	$200:1:2 \times 10^{-4}$	DMA	BTPA	1	3	93	23 740	18 430	1.09
14	$200:1:2 \times 10^{-4}$	NIPAAm	BTPA	1	3	95	21 700	21 400	1.08
15	$200:1:10 \times 10^{-4}$	isoprene	BTPA	5	12	23	6200	3200	1.35

[a]The reactions were performed at room temperature under 4.8 W blue LED light (λ_{max} = 435 nm). [b]Monomer conversion for MA determined by ^{1}H NMR spectroscopy was calculated by the following equation: $\alpha = (1 - [(I^{5.5-6.0ppm}/2)/(I^{3.5ppm}/3)]) \times 100$. [c]Theoretical molecular weight calculated using the following equation: $M_{n,th} = [M]_0/[thiocar]_0 \times MW^M \times \alpha + MW^{thiocar}$, where $[M]_0$, $[thiocar]_0$, MW^M, α, and $MW^{thiocar}$ correspond to monomer and thiocarbonylthio compound concentration, molar mass of monomer, monomer conversion, and molar mass of thiocarbonylthio compound. [d]Molecular weight and polydispersity determined by GPC analysis. [e]Molecular weight determined by ^{1}H NMR using $M_{n,NMR} = (I^{3.8ppm}/1)/(I^{7.8ppm}/2) \times MW^{HPMA} + MW^{CPADB}$, where $I^{3.8ppm}$ and $I^{7.8ppm}$ correspond to integrals of signal at δ 3.8 ppm and δ 7.8 ppm attributed to CH of HPMA and phenyl group (Z-group) of CPADB. [f]PSt phase separates at high monomer conversion in DMSO due its poor solubility in this solvent, resulting in a slight increase of M_w/M_n.

Table 3. Examples of Polymers Synthesized Using Unconjugated Monomers in This Study

no.	exp. cond.[a] [M]:[thiocar]:[Ir]	monomer	thiocar	[Ir]/[M] (ppm)	time (h)	α[b] (%)	$M_{n,th}$[c] (g/mol)	$M_{n,GPC}$[d] (g/mol)	M_w/M_n
1	$200:1:40 \times 10^{-4}$	VAc	BTPA	20	24	0			
2	$200:1:40 \times 10^{-4}$	VAc	xanthate	20	22	76	13 300	18 200	1.20
3	$200:1:10 \times 10^{-4}$	VAc	xanthate	5	2	16	3700	5300	1.09
4	$200:1:10 \times 10^{-4}$	VAc	xanthate	5	24	81	14 000	18 300	1.20
5	$200:1:2 \times 10^{-4}$	VAc	xanthate	1	20	41	7200	11 900	1.18
6	$1000:1:50 \times 10^{-4}$	VAc	xanthate	5	22	ND[e]	ND[e]	56 000	1.38
7	$200:1:10 \times 10^{-4}$	VP	xanthate	5	3	22	4500	3800	1.18
8	$200:1:10 \times 10^{-4}$	VP	xanthate	5	24	80	20 800	22 000	1.38
9	$100:1:10 \times 10^{-4}$	DVP	xanthate	10	6	22	3100	3500	1.27
10	$100:1:10 \times 10^{-4}$	DVP	xanthate	10	14	41	5800	6700	1.17
11	$170:1:17 \times 10^{-4}$	NVP	xanthate	10	6	40	6900	7200	1.23
12	$170:1:17 \times 10^{-4}$	NVP	xanthate	10	14	65	12 500	13 200	1.10

[a]The reactions were performed at room temperature under 4.8 W blue LED light (λ_{max} = 435 nm). [b]Monomer conversion determined by ^{1}H NMR spectroscopy. [c]Theoretical molecular weight calculated using the following equation: $M_{n,th} = [M]_0/[xanthate]_0 \times MW^M \times \alpha + MW^{xanthate}$, where $[M]_0$, $[xanthate]_0$, MW^M, α, and $MW^{xanthate}$ correspond to M and xanthate concentration, molar mass of M, monomer conversion, and molar mass of xanthate. [d]Molecular weight and polydispersity determined by GPC analysis. [e]ND: not determined.

this technique (Supporting Information, Table S1). To confirm that the activation and deactivation is induced only by the catalyst under light, control experiments in the absence of catalyst (Table 1, no. 6) or light (data not shown) were conducted. Polymerization was not detected in either case.

dx.doi.org/10.1021/ja501745g | J. Am. Chem. Soc. 2014, 136, 5508−5519

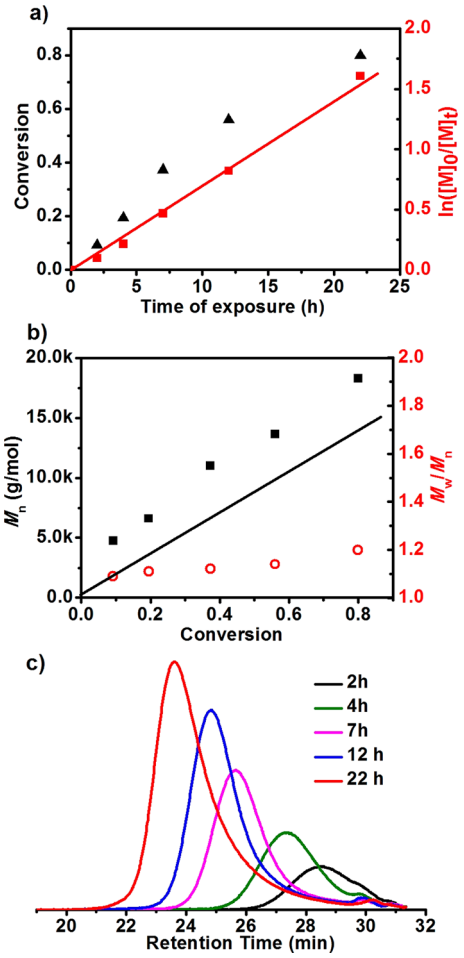

Figure 4. Photopolymerization of VAc in the presence of xanthate and *fac*-[Ir(ppy)$_3$] as photoredox catalyst under 4.8 W blue LED irradiation at room temperature: (a) monomer conversion (▲) and $\ln([M]_0/[M]_t)$ (■) versus time; (b) $M_{n,GPC}$ (■), $M_{n,th}$ (black line), and M_w/M_n (○) versus conversion; and (c) GPC traces at different times of exposure. Experimental condition: [VAc]:[xanthate]:[catalyst] = 200:1:10 × 10^{-4}.

Subsequently, to demonstrate temporally controlled polymerization, the mixture of MMA, CPADB, and catalyst was exposed to an alternating light "ON" and "OFF" environment. In the absence of light (light "OFF"), no polymerization was observed. When the light was "ON", the polymerization proceeded as expected (Figure 2a). A short inhibition period (typically 3 h) was observed for MMA, which could be attributed to traces of impurity in RAFT compound or to the slow fragmentation of the dithiobenzoates similar to traditional RAFT processes.[43−46] Further investigations on this inhibition period will be carried out in the future. The monomer conversion as well as $\ln([M]_0/[M]_t)$ increased with the exposure time to light, indicating a controlled/living polymerization mechanism (Figure 2c).[47] The plot of $M_{n,GPC}$ versus monomer conversion gave a linear relationship (Figure 2b) in good agreement with the theoretical values ($M_{n,th}$) and molecular weights calculated by NMR ($M_{n,NMR}$). Gel permeation chromatography (GPC) analysis revealed a narrow MWD (Figure 2d). Additional kinetics, with different molar ratios of [catalyst]:[MMA] ranging from 5 to 1 ppm, were reported (Figure 3A and Supporting Information, Figure S4). As expected, the increase of catalyst accelerated polymerization rates with little effect on the polydispersities and the control of molecular weights. In contrast to the radical initiators used in conventional RAFT and ATRP polymerization, the amount of catalyst employed in photoinduced living polymerization is much lower with a typical ratio of 1 ppm catalyst relative to monomer. For instance, ATRP[48−50] or single electron transfer-living radical polymerization (SET-LRP)[12,51,52] typically employs a ratio of [monomer]:[copper] equal to 100:1[48] (except in the case of activator regenerated by electron transfer (ARGET-ATRP) ATRP, where a lower ratio can be employed under specific conditions),[53−55] while in the RAFT process a ratio of [thiocarbonylthio]:[initiator] equal to 100:10 is commonly employed.[22−24,50,56−60] To further explore the efficiency of the catalyst, the light intensity was varied from 1.0 to 4.8 W. Although lower light intensities (1.0 and 2.4 W) resulted in both a slight increase of the inhibition period and a slight decrease in the polymerization rate (Figure 3B), the polymerizations still exhibited good control of the molecular weights and polydispersities (<1.15), indicating that light intensity can be manipulated to regulate the polymerization rates. In contrast to previous works on photopolymerizations employing light intensity ranging from 10 to 100 W,[3,4,8,9,19,20,25] our work is the first example to use a light intensity lower than 5 W. Low light intensity is highly beneficial for the reduction of energy usage and also aids in decreasing the occurrences of side reactions or the degradation of specific functionalities. Additionally, the wavelength of light source was varied from 500 nm (green LED) to 700 nm (red LED), and no polymerization was observed as expected.

PMMA polymers obtained using photoinduced living polymerization were purified, and analyzed via ^{1}H NMR, UV−vis spectroscopy, and GPC using dual UV (λ = 305 nm) and RI detectors. The signals at δ 7.3, 7.4, and 7.8 ppm characteristic of the phenyl group in the ^{1}H NMR spectrum (Supporting Information, Figure S5) and the signal at 305 nm characteristic of the C═S bond in the UV−vis spectrum[61] (Supporting Information, Figure S6) confirmed the presence of the dithiobenzoate end-group. Both UV and RI detectors of GPC showed similar MWDs, which also demonstrated the presence of the dithiobenzoate functionality (Supporting Information, Figure S7). In addition, CPADB was exposed under blue LED light in the presence of catalyst and absence of monomer for 24 h as a control experiment, to test their compatibility. ^{1}H NMR analysis did not show any degradation or formation of side products (Supporting Information, Figure S8).

To further investigate the end-group fidelity, chain extensions of PMMA polymers were carried out using MMA, oligoethylene glycol methyl ether methacrylate (OEGMA), and *tert*-butyl methacrylate (*t*BuMA) as monomers to yield diblock copolymers: PMMA-*b*-PMMA, PMMA-*b*-POEGMA, and PMMA-*b*-P*t*BuMA (Supporting Information, Scheme S3). GPC revealed a complete shift of the starting macroinitiators to lower retention time with low M_w/M_n values (<1.15) (Supporting Information, Figures S9−11 and Table S3). To illustrate the exceptional retention of the end-group fidelity and the versatility of this polymerization technique, we decided to prepare PMMA-*b*-PMMA-*b*-PMMA triblock copolymers with ultrahigh molecular weight (M_n > 300 000 g/mol) using PMMA macroinitiator with a molecular weight of 20 200 g/mol. GPC showed the formation of well-defined blocks with unprecedented control (M_n = 350 200 g/mol, M_w/M_n = 1.30) for PMMA (Supporting Information, Figure S12). This is the

dx.doi.org/10.1021/ja501745g | J. Am. Chem. Soc. 2014, 136, 5508−5519

Table 4. Molecular Weights and Polydispersities (M_w/M_n) of Block Copolymers Synthesized by Photoinduced Living Polymerization Using PMMA, PHPMA, PSt, PDMA, PMA, and PNVP as Macroinitiators[a]

no.	copolymers	conversion[b] (%)	$[M]_0/[macro]_0$[c]	$M_{n,th}$[d] (g/mol)	$M_{n,GPC}$[e] (g/mol)	M_w/M_n
1	PMMA macroinitiator				13 800	1.08
2	PMMA-*b*-PSt	0	200/1			
3	PMMA-*b*-PMA	0	200/1			
4	PMMA-*b*-PHPMA	38	200/1	25 100	31 330	1.16
5	PHPMA macroinitiator				58 600 (24 210)[f]	1.16
6	PHPMA-*b*-PSt	0	200/1			
7	PHPMA-*b*-PMMA	83	200/1	78 600	75 200	1.13
8	PSt macroinitiator				4300	1.09
9	PSt-*b*-PMMA	41	200/1	12 200	105 000	2.1
10	PSt-*b*-PMA	85	400/1	34 800	35 400	1.20
11	PMA macroinitiator				12 600	1.08
12	PMA-*b*-PDMA	72	400/1	41 500	40 300	1.11
13	PMA-*b*-PSt	24	200/1	18 600	17 200	1.11
14	PDMA macroinitiator				18 430	1.09
15	PDMA-*b*-PMA	56	400/1	36 800	37 300	1.14
16	PDMA-*b*-PSt	58	400/1	41 700	42 800	1.28
17	PNVP macroinitiator				7200	1.23
18	PNVP-*b*-PVAc	35	200/1	12 200	13 300	1.24

[a]The reactions were performed in DMSO at room temperature using 4.8 W blue LED lamp (λ_{max} = 435 nm) as light source and molar ratio [M]/[catalyst] = 200:10 × 10^{-4} (styrene case: [M]/[catalyst] = 400:80 × 10^{-4}). [b]Monomer conversion determined by ^{1}H NMR spectroscopy. [c]Molar ratio of monomer to macroinitiator. [d]Theoretical molecular weight calculated using the following equation: $M_{n,th}$ = $[monomer]_0/[polymer\text{-}macro]_0$ × $MW^{monomer}$ × α + $MW^{Pplymer\text{-}macro}$, where $[monomer]_0$, $[polymer\text{-}macro]_0$, $MW^{monomer}$, α, and $MW^{Pplymer\text{-}macro}$ correspond to monomer and polymer macroinitiator concentration, molar mass of monomer, monomer conversion, and molar mass of polymer macroinitiator. [e]Molecular weight and polydispersity determined by GPC analysis. [f]Molecular weight calculated by NMR (see Table 2 footnote).

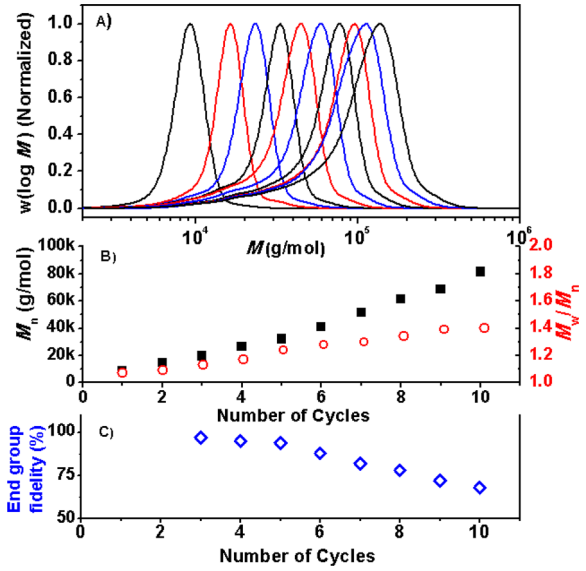

Figure 5. Multiblock copolymers obtained by photoinduced living polymerization using 4.8 W blue LED lamp (λ_{max} = 435 nm) as light source. (A) MWDs of different block copolymers; (B) evolution of number-average molecular weights (■) and M_w/M_n (○) versus number of chain extension cycles; and (C) evolution of end-group fidelity versus number of chain extension.

first example of photocontrolled polymerization demonstrating the synthesis of high molecular weight of poly(methacrylate) block copolymers. Such block copolymers have rarely been reported in the literature,[62] as it is well-known that methacrylate monomers are difficult to control via controlled/living free radical polymerization (C/LRP) at high molecular weight (M_n > 100 000 g/mol).

3. Polymerization of Other Conventional Conjugated Monomers, Including Acrylate, (Meth)acrylamide, Styrene, and Isoprene by Photoinduced Living Polymerization. Following the study of photoinduced living polymerization on MMA, we decided to test the application of this technique for the polymerization of other common monomers, such as styrene (St), acrylate (methyl acrylate (MA)), *tert*-butyl acrylate (*t*BA), oligo(ethylene glycol) methyl ether acrylate (OEGA, average M_n 480), *N*-(2-hydroxylpropyl) methacrylamide (HPMA), *N*-isopropylacrylamide (NIPAAm), *N*,*N*-dimethylacrylamide (DMA), and isoprene. The first attempts to polymerize St, MA, and DMA were unsuccessful using CPADB in DMSO (data not shown). In the case of HPMA, we observed the formation of polymers with a good MWD (M_w/M_n < 1.10, Table 2, nos. 1−3). The molecular weights determined by ^{1}H NMR were in very good agreement with the theoretical values (Supporting Information, Figure S13). However, we observed that the theoretical molecular weights were much lower than that measured by GPC, which could be attributed to a difference in the hydrodynamic volumes between the PSt standard and PHPMA polymer. Such observations have been previously reported in the literature.[63]

To polymerize St, MA, and DMA, we decided to test a trithiocarbonate compound (BTPA) instead of the dithiobenzoate compound (CPADB). The initial attempts using the trithiocarbonate revealed the formation of polymers with conversions greater than 90% for MA and DMA in 2 and 3 h, respectively, and 50% for St in 48 h (Table 2, nos. 4, 11, and 13). $M_{n,GPC}$'s were in good agreement with $M_{n,th}$ with narrow MWDs (M_w/M_n < 1.17) demonstrating that the polymerizations were well controlled. Following these successful tests, the catalyst concentration was reduced for MA to 0.2 and 0.1 ppm (Table 2, nos. 6 and 7). At 0.2 ppm, a monomer conversion of 96% was observed after 10 h, showing that the

dx.doi.org/10.1021/ja501745g | J. Am. Chem. Soc. 2014, 136, 5508−5519

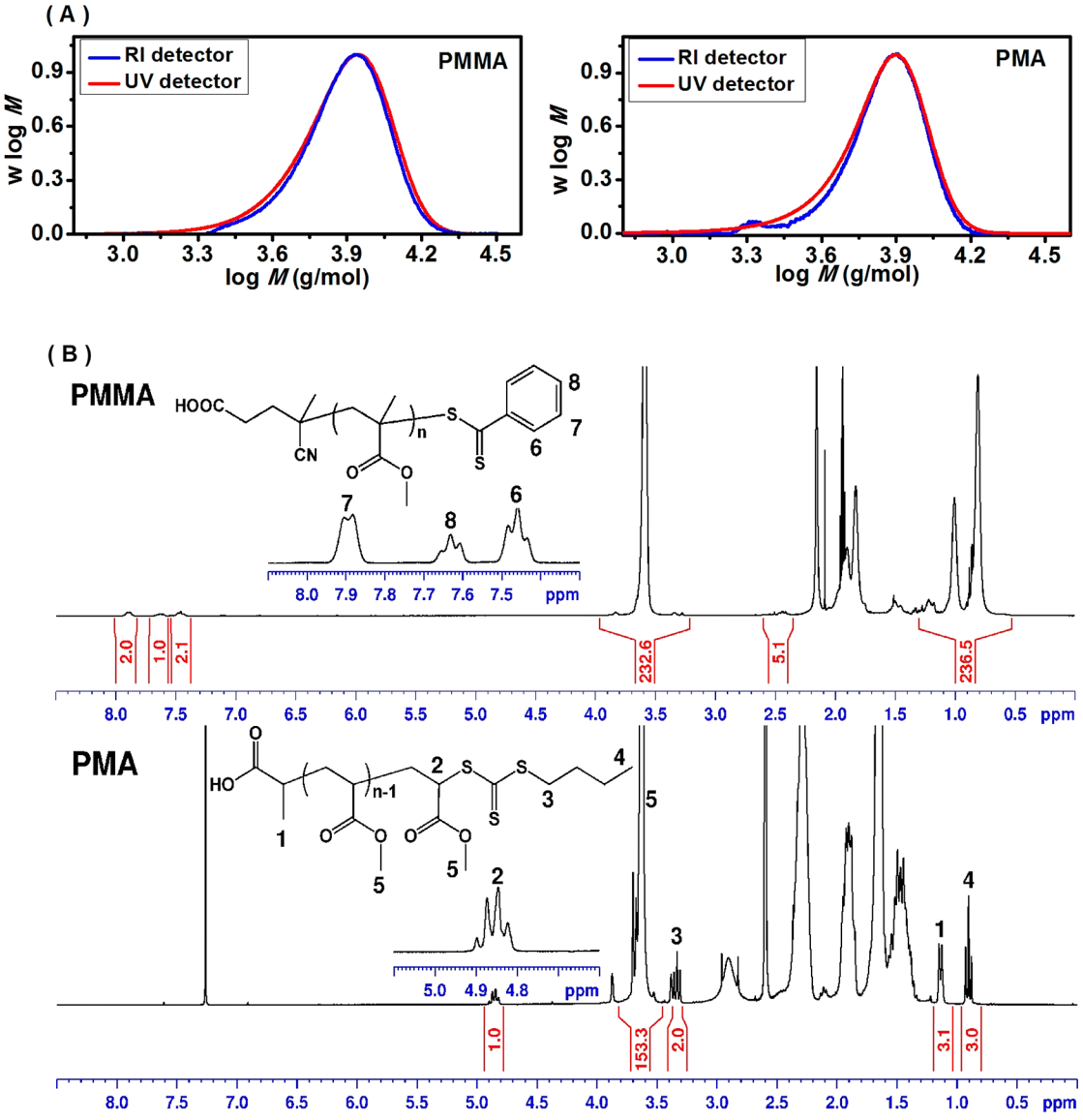

Figure 6. (A) Comparison of molecular weight distributions recorded using a RI and UV (λ = 305 nm) detector and (B) ^{1}H NMR spectra for purified PMMA and PMA polymer synthesized by photoinduced living polymerization in the presence of air using BTPA and 4.8 W blue LED lamp (λ_{max} = 435 nm) as light source ($M_{n,NMR,PMMA}$ = 8010 g/mol, $M_{n,GPC,PMMA}$ = 8200 g/mol, monomer conversion 41%; $M_{n,NMR,PMA}$ = 4620 g/mol, $M_{n,GPC,PMA}$ = 4700 g/mol, monomer conversion 29%).

polymerization of MA can be carried out using an ultralow concentration of catalyst. As expected, at lower catalyst concentration (0.1 ppm), the polymerization required longer reaction time to reach high monomer conversion. Additionally, a lower catalyst concentration resulted in a slight increase of the PDI.

Subsequently, the concentration of BTPA was varied to prepare PMA polymers with different molecular weights ranging from 2000 to 2 000 000 g/mol (Supporting Information, Table S4). To our knowledge, the synthesis of high molecular weight polyacrylate polymers using controlled/living radical polymerization techniques, including RAFT, ATRP, and NMP, is challenging and has only been successfully reported by a limited number of specific techniques.[52,64−66] To confirm the presence of the trithiocarbonate end-group, PMA with molecular weight of 8000 g/mol was purified and analyzed by ^{1}H NMR (Supporting Information, Figure S15) and UV−vis spectroscopy (Supporting Information, Figures S16 and S17). All three techniques displayed high end-group fidelity (~100%). The controlled/living character was further demonstrated by monitoring monomer conversion and molecular weight versus exposure time for both MA and St (Supporting Information, Figures S14 and S18). ^{1}H NMR, GPC using RI and UV detector, and UV−vis were also employed to confirm the presence of trithiocarbonate end-group for a PSt polymer (Supporting Information, Figures S19,20). In addition, good control of the molecular weight and a narrow MWD was also noted for BSTP (Table 2, no. 8) with a polymerization rate comparable to that of BTPA, suggesting that this polymerization has the potential to utilize a broad variety of trithiocarbonate compounds. Other acrylic monomers, such as OEGA and *t*BA, were also successfully polymerized using this technique (Table 2, nos. 9,10). Subsequently, styrene was investigated using different concentrations of catalyst. The polymerization of styrene required a high amount of photoredox catalyst to reach high conversion. We attributed the slow

dx.doi.org/10.1021/ja501745g | J. Am. Chem. Soc. 2014, 136, 5508−5519

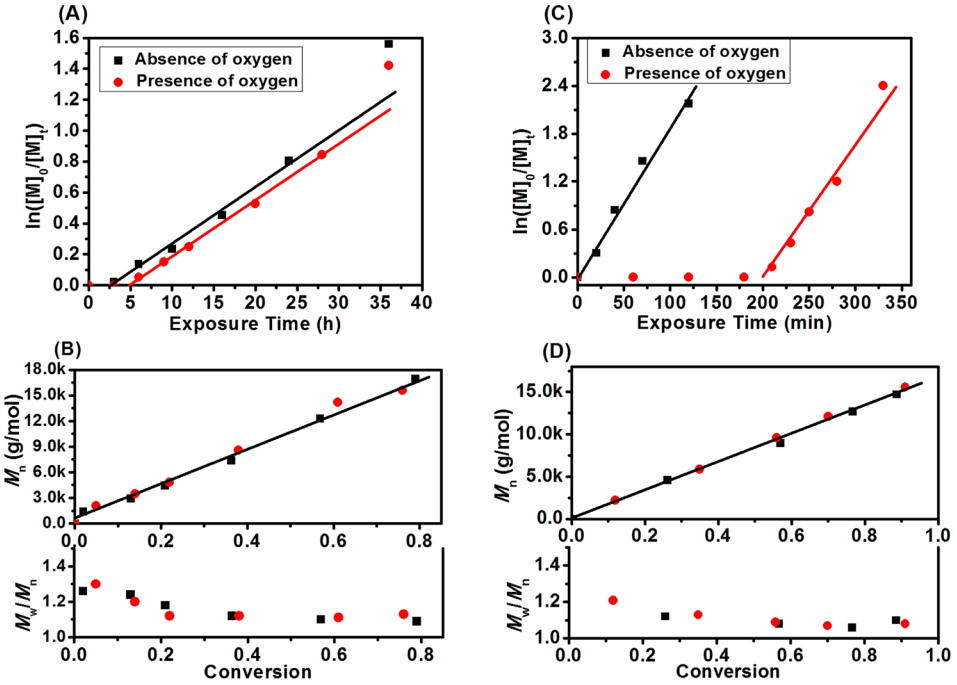

Figure 7. Kinetics plots for photoinduced living polymerizations of MMA (A and B) and MA (C and D) in the presence of oxygen (red ●) and absence of oxygen (■) in DMSO. (A) $\ln([M]_0/[M]_t)$ versus exposure time for MMA; (B) M_n versus conversion (top) and M_w/M_n versus conversion (bottom) for MMA; (C) $\ln([M]_0/[M]_t)$ versus exposure time for MA; and (D) M_n versus conversion (top) and M_w/M_n versus conversion (bottom) for MA. Note: $[M]_0$ and $[M]_t$ correspond to the concentrations of monomers at time zero and t, respectively. (B and D) Straight lines correspond to the theoretical values.

polymerization of styrene to its low propagation rate constant (k_p) at room temperature. However, at high conversion, we observed that PSt precipitated in DMSO due to its poor solubility in this solvent. Nevertheless, good control was still achieved. In contrast, acrylamide, including DMA and NIPAAm, was rapidly polymerized in 3 h (close to full monomer conversion) using a very low amount of catalyst (1 ppm relative to monomer). As indicated by GPC and NMR, the molecular weights were well controlled with a narrow MWD ($M_w/M_n < 1.10$). Finally, isoprene (Table 2, no. 15) was investigated using BTPA as initiator and chain transfer agent in the presence of photoredox catalyst (5 ppm). After 12 h, we observed a conversion of 23% determined by NMR, while GPC revealed the synthesis of polyisoprene with a molecular weight of 3200 g/mol (and M_w/M_n of 1.35), which demonstrates that this process is very efficient for the polymerization of conjugated monomers.

4. Polymerization of Unconjugated Monomers, Including Vinyl Acetate (VAc), Vinyl Pivalate (VP), *N*-Vinyl Pyrrolidinone (NVP), and Dimethyl Vinylphosphonate (DVP), by Photoinduced Living Polymerization. We decided to investigate unconjugated monomers using our process. In this work, we selected four different model monomers, including vinyl acetate (VAc), vinyl pivalate (VP), *N*-vinylpyrrolidinone (NVP), and dimethyl vinylphosphonate (DVP). All of these monomers are widely employed in industry due to their interesting properties. For instance, PVAc is the precursor of polyvinyl alcohol (used in coatings and also a biocompatible polymer), and PNVP is used in the synthesis of inks, coatings, and adhesives. First, vinyl acetate (VAc) was investigated using BTPA or xanthate in the presence of various photoredox catalyst concentrations. Initial polymerizations using BTPA as initiator and chain transfer agent were unsuccessful (Table 3, no. 1). However, successful polymerizations were obtained with xanthate (Table 3, nos. 2–6). The experimental molecular weights determined by GPC were greater than the theoretical values, which was attributed to the difference in hydrodynamic volume between PVAc and the PSt standard. NMR was invoked to calculate the molecular weight. $M_{n,NMR}$ was in good agreement with the theoretical values. Interestingly, the amount of photoredox catalyst does not affect the molecular weight distribution, as all of the polymerizations displayed a PDI lower than 1.20. After these initial successful results, VAc kinetics was investigated using [*fac*-[Ir(ppy)$_3$]]/[monomer] of 5 ppm. A linear evolution of $\ln([M]_0/[M_t])$ and molecular weight versus exposure time demonstrates the living character of this polymerization (Figure 4). To demonstrate the presence of xanthate end-group, PVAc (Table 3, nos. 2 and 3) was analyzed by NMR (Supporting Information, Figure S21) and GPC equipped with RI and UV detector (Supporting Information, Figure S22). Other monomers, including vinyl pivalate (VP), *N*-vinyl pyrrolidinone (NVP), and dimethyl vinylphosphonate (DVP), were also tested using a catalyst concentration of 10 ppm (relative to monomer). These monomers revealed the synthesis of polymers with a narrow MWD and good control of the molecular weight (Table 3, nos. 7–12). These results demonstrate that this polymerization technique can control a diverse range of unconjugated monomers.

5. Synthesis of Diblock Copolymers Using Different Monomer Families. To investigate the versatility of this approach, we decided to prepare block polymers comprised of different monomer families. Six different macroinitiators, that is, PMMA, PHPMA, PSt, PMA, PDMA, and PNVP, were prepared by photoinduced living polymerization, and subsequently purified by precipitation (Table 4). First, the PMMA

dx.doi.org/10.1021/ja501745g | J. Am. Chem. Soc. 2014, 136, 5508–5519

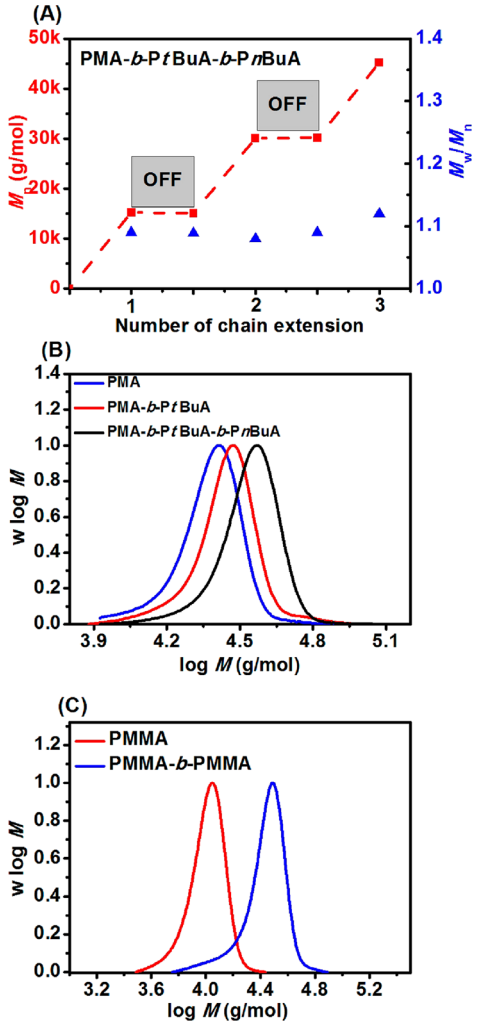

Figure 8. Preparation of block copolymers in the presence of oxygen. (A) The "ON"/"OFF" experiment for preparing triblock copolymer PMA-*b*-P*t*BuA-*b*-P*n*BuA; (B) molecular weight distributions of triblock copolymer PMA-*b*-P*t*BuA-*b*-P*n*BuA; and (C) molecular weight distribution of diblock of PMMA-*b*-PMMA.

macroinitiator was prepared using CPADB and chain extended in the presence of St, MA, and HPMA using a concentration of photoredox catalyst of 5 ppm relative to the monomer. Surprisingly, the chain extensions of PMMA with St and MA were unsuccessful, as NMR and GPC did not reveal monomer conversion or a shift of MWD, respectively. This is a major difference between our process and conventional RAFT or ATRP polymerization techniques. Indeed, PMMA can be easily chain extended with MA and St using the conventional RAFT polymerization process. One possible explanation is that the photoredox catalyst cannot activate PMA−S(C═S)−Ph end-group. Nevertheless, the chain extension of PMMA with HPMA was successful via photoinduced living polymerization, resulting in the synthesis of PMMA-*b*-HPMA with a narrow MWD (M_w/M_n < 1.2) (Table 4, no. 4 and Supporting Information, Figure S24). PHPMA was also successfully chain extended in the presence of MMA to yield PHPMA-*b*-PMMA diblock copolymer (Table 4, no. 7 and Supporting Information, Figure S25).

The chain extension of PSt macroinitiator with MMA was uncontrolled, resulting in a much higher molecular weight polymer than the theoretical values with a broad MWD (Table 4, no. 9). Such results have been previously reported in the literature for RAFT and ATRP process and are attributed to the difference in reactivity between the end-groups (PMMA-RAFT and PSt-RAFT). Successful chain extension of PSt with MA was confirmed by GPC with a narrow MWD (M_w/M_n = 1.20) (Table 4, no. 10 and Supporting Information, Figure S26).

As expected, the chain extensions of PMA and PDMA were successful with MA, DMA, and St to yield well-defined PMA-*b*-PDMA, PMA-*b*-PSt, PDMA-*b*-PMA, and PDMA-*b*-PSt block copolymers, respectively (Table 4, nos. 12, 13, 15, and 16, and Supporting Information, Figures S27−30). Finally, the synthesis of PNVP-*b*-PVAc was achieved using catalyst concentration of 10 ppm relative to monomer (Table 4, no. 18 and Supporting Information, Figure S31).

6. Synthesis of Multiblock Copolymers via Photoinduced Living Polymerization. To further investigate the robustness of the catalyst, successive chain extensions of PMA were performed to generate a decablock $P(MA)_{10}$ copolymer without supplementary addition of catalyst. We first synthesized a PMA macroinitiator ($M_{n,GPC}$ = 8560 g/mol) by polymerization of MA in the presence of BTPA and 5 ppm of catalyst for 2 h in DMSO. NMR confirmed full monomer conversion (>98%) in the first step. For the second block, MA in a degassed DMSO solution was then added under nitrogen to the macroinitiator, and the polymerization was allowed to continue for a further 4 h to reach full monomer conversion (Supporting Information, Table S5). This process was repeated several times until the formation of the high-order multiblock polymers with high molecular weight ($M_{n,GPC} \approx$ 82 000 g/mol, $M_w/M_n \approx$ 1.40) was obtained (Figure 5). To our knowledge, this is the first time that such high molecular weight block copolymers were obtained using an iterative approach under light. In previous studies, short block polymers, with a typical $M_{n,block}$ ranging from 500 to 5000 g/mol, were achieved using conventional C/LRP (copper(0)-mediated polymerization and RAFT polymerization).[67,68]

GPC analysis of the MWDs confirmed successful chain extensions as manifested by clear shifts to higher molecular weights in each step. In addition, the MWD remained narrow ($M_w/M_n \approx$ 1.40) even after 10 chain extensions (Figure 5B). $M_{n,GPC}$'s were in good agreement with the theoretical values, although the formation of some low molecular weight tailings was observed after 4−5 cycles (Figure 5A). Semiquantitative analysis using GPC traces was also employed to estimate the proportion of dead polymers after each chain extension using a previously published procedure.[68,69] The method is based on the hypothesis that the low molecular weight tails are attributed to the dead polymers. To estimate the living chains by using this method, we converted the molecular weight distributions to the corresponding number distributions (Supporting Information, Figure S32). Figure 5C showed the plot of livingness versus number of chain extensions. Unfortunately, we observed a gradual decrease of the livingness after each cycle. Nevertheless, the livingness (i.e., number of living polymer chains) was greater than 65% after 10 chain extensions, which represent almost 90 wt % of living polymer. This is a remarkable result considering the lack of optimizations to the system, that is, concentration of catalyst, light intensity, and polymerization time. In conventional controlled radical polymerization techniques, the livingness is usually less than 90% for each chain extension.[68−70] These experimental results demonstrate the extreme robustness and efficiency of the

dx.doi.org/10.1021/ja501745g | J. Am. Chem. Soc. 2014, 136, 5508−5519

catalyst in this photoinduced living polymerization to make multiple chain extensions.

7. Polymerization in the Presence of Air. Another unique property of this process is the possibility to perform the polymerization without degassing the reaction mixtures. It is well-known that oxygen is detrimental to radical polymerizations, as oxygen is an excellent radical scavenger. Conventional free radical and controlled/living radical polymerization techniques, including ATRP,[49,50] RAFT,[57] and NMP,[70] are susceptible to trace amounts of oxygen and require deoxygenation procedures, such as degassing with nitrogen or several freeze−pump−thaw cycles (except for ARGET,[71−73] SET-LRP,[64,74,75] and SARA process;[76] however, these techniques require specific conditions and can only polymerize a narrow range of monomer families (i.e., usually acrylate)). Construction of an oxygen-free environment could be challenging for specific industrial applications, such as surface modifications, miniemulsion polymerization, coatings, etc. We hypothesized that the excellent reductive qualities of *fac*-[Ir(ppy)$_3$] catalyst would be able to overcome the lack of deoxygenation by reducing oxygen into inactive species. As the redox potential of O_2 in acetonitrile in the presence of water is around +1.23 V,[77,78] we hypothesized that the reduction of oxygen into hydroxide ion (OH) was possible in our system. In a closed and sealed vessel, the oxygen would slowly be consumed and eliminated, while a small amount of hydroxide ion will be produced as a side product.

In our first attempts, we decided to test our hypothesis for the polymerization of MMA and MA. The polymerizations of MMA and MA were performed in a sealed but nondegassed vessel of 4 mL using a total liquid volume of 3 mL (50/50 (v/v) of solvent/monomer) under a 4.8 W blue LED light. After 24 h, the reaction solutions were analyzed by ^{1}H NMR and GPC. NMR revealed a monomer conversion of 99% and 50% for MA and MMA, respectively, while GPC showed the presence of PMA and PMMA with very good control of the molecular weight in good agreement with the theoretical values and M_w/M_n (<1.10). Additional analyses for lower molecular weights using GPC equipped with a dual UV and RI detectors revealed the presence of identical MWDs, demonstrating the homogeneous proportion of thiocarbonylthio groups within the polymer chains (Figure 6A). ^{1}H NMR and UV−vis analyses were invoked to quantify the exact amounts of dithiobenzoate and trithiocarbonate group present in both polymers after purification. Figure 6B displays the ^{1}H NMR spectra of purified PMMA and PMA synthesized without prior degassing. Dithiobenzoate and trithiocarbonate groups were confirmed by the characteristic signals at δ 7.3−7.8 ppm and δ 4.8 ppm, respectively, which could be used to calculate the molecular weights of polymers. Both NMR and GPC values for molecular weights were in good agreement, demonstrating high end-group fidelity. Finally, the molecular weights were also calculated by UV−vis using the signal at 305 nm and the extension coefficients of dithiobenzoate and trithiocarbonate (data not shown), which were also in good agreement with $M_{n,th}$ and $M_{n,GPC}$.

On the basis of these preliminary results, we decided to investigate the polymerization kinetics of MMA and MA. As expected, a long inhibition period of 3−4 h was observed attributed to the reduction of oxygen by the photoredox catalyst. After this inhibition period, the polymerization proceeded in a controlled manner, giving linear plots of M_n versus monomer conversion and $\ln([M]_0/[M]_t)$ versus exposure time (Figure 7A and C). Interestingly, the slopes of $\ln([M]_0/[M]_t)$ (apparent propagation constant, k_p^{app}) versus time for the polymerizations in the presence of air were almost the same as the degassed reactions after the inhibition period (Figure 7A and C), which indicated that both photocatalyst and thiocarbonylthio compounds were not degraded during the oxygen reduction period. In addition, the evolutions of $M_{n,GPC}$ values versus exposure time were in good agreement with those in the absence of oxygen (degassed system) and theoretical values (Figure 7B and D). GPC showed a shift of the molecular weight distribution to higher molecular weight with a narrow polydispersity (Supporting Information, Figure S33). To further investigate the livingness (i.e., the end-group fidelity) and the robustness of the catalyst in a nondegassed environment, successive chain extensions of PMA and PMMA were performed to generate a diblock of PMMA-*b*-PMMA and a triblock of PMA-*b*-P*t*BuA-*b*-P*n*BuA copolymers without degassing the solutions (Figure 8). In this approach, we decided to use an iterative process as described in the previous paragraph. To our knowledge, it is the first time that block copolymers were obtained without purification and also degassing between each chain extension. For each chain extension, we added a nondegassed solution containing monomer and solvent. Subsequently, the solution was placed under a 4.8 W blue LED light for 7 h (MA) and 24 h (MMA) to obtain high monomer conversion (>98% determined by ^{1}H NMR). The solutions then were placed in the dark to avoid the formation of dead polymers during monomer conversion analysis. After confirmation of full monomer conversion, a new aliquot of monomer and solvent was added to the mixture. After an inhibition period of 2−3 h, the polymerization proceeded until full monomer conversion. GPC revealed the formation of well-defined block copolymers with a narrow MWD (M_w/M_n < 1.10). Purified copolymers were finally analyzed by NMR to determine the exact composition (Supporting Information, Figure S34).

CONCLUSION

We report a robust and highly efficient photoinduced living polymerization, which is able to control a large range of monomer families (methacrylates, acrylates, styrene, vinyl ester, methacrylamide, and acrylamide). This polymerization technique presents greater advantages over conventional C/LRP techniques, as it can be used to prepare polymers with molecular weights ranging from 1000 to 2 000 000 g/mol and narrow molecular weight distributions while maintaining high end-group fidelity. More importantly, the polymerization can be performed in the presence of air, as the photoredox catalyst has the ability to reduce oxygen into inactive species. Another distinguishing feature of this technique is that the polymerization can be activated and regulated at ultralow concentrations of photocatalyst (*fac*-[Ir(ppy)$_3$]) (ppm range) under low intensity blue LED light (1−4.8 W, λ_{max} = 435 nm). The accessibility of the end-groups (dithiobenzoate or trithiocarbonate) was confirmed by multiple chain extensions to yield multiblock copolymers with high purity and lack of supplementary addition of catalyst. As iridium-based catalysts are expensive due to the rarity of Ir, this process was tested with other commonly used photoredox catalysts, such as Ru(bpy)$_3$Cl$_2$, and an inexpensive organocatalyst (Fluorescein) for the photocontrolled polymerization of methyl methacrylate, methyl acrylate and styrene in the presence of thiocarbonylthio compounds. Successful polymerizations were observed (Sup-

dx.doi.org/10.1021/ja501745g | J. Am. Chem. Soc. 2014, 136, 5508−5519

porting Information, Table S6), which demonstrates the viability of this method even when less efficient catalysts are used. Further studies are still in progress.

■ ASSOCIATED CONTENT

Supporting Information

Experimental details, fluorescence spectrum, UV−vis spectra, NMR spectra, and GPC traces (Figures S1−S34, Tables S1−S6, and Schemes S1−S3). This material is available free of charge via the Internet at http://pubs.acs.org.

■ AUTHOR INFORMATION

Corresponding Author

cboyer@unsw.edu.au

Notes

The authors declare no competing financial interest.

■ ACKNOWLEDGMENTS

We thank UNSW for funding. C.B. acknowledges the Australian Research Council (ARC) for his Future Fellowship.

■ REFERENCES

(1) Bortolamei, N.; Isse, A. A.; Magenau, A. J. D.; Gennaro, A.; Matyjaszewski, K. *Angew. Chem., Int. Ed.* **2011**, *50*, 11391−11394.

(2) Magenau, A. J. D.; Strandwitz, N. C.; Gennaro, A.; Matyjaszewski, K. *Science* **2011**, *332*, 81−84.

(3) Fors, B. P.; Hawker, C. J. *Angew. Chem., Int. Ed.* **2012**, *51*, 8850−8853.

(4) Ciftci, M.; Tasdelen, M. A.; Yagci, Y. *Polym. Chem.* **2014**, *5*, 600−606.

(5) Tehfe, M.-A.; Ma, L.; Graff, B.; Morlet-Savary, F.; Fouassier, J.-P.; Zhao, J.; Lalevée, J. *Macromol. Chem. Phys.* **2012**, *213*, 2282−2286.

(6) Lalevée, J.; Peter, M.; Dumur, F.; Gigmes, D.; Blanchard, N.; Tehfe, M.-A.; Morlet-Savary, F.; Fouassier, J. P. *Chem.—A Eur. J.* **2011**, *17*, 15027−15031.

(7) Pierre Fouassier, J.; Lalevee, J. *RSC Adv.* **2012**, *2*, 2621−2629.

(8) Lalevée, J.; Tehfe, M.-A.; Dumur, F.; Gigmes, D.; Blanchard, N.; Morlet-Savary, F.; Fouassier, J. P. *ACS Macro Lett.* **2012**, *1*, 286−290.

(9) Fors, B. P.; Poelma, J. E.; Menyo, M. S.; Robb, M. J.; Spokoyny, D. M.; Kramer, J. W.; Waite, J. H.; Hawker, C. J. *J. Am. Chem. Soc.* **2013**, *135*, 14106−14109.

(10) Zhou, H.; Johnson, J. A. *Angew. Chem., Int. Ed.* **2013**, *52*, 2235−2238.

(11) Poelma, J. E.; Fors, B. P.; Meyers, G. F.; Kramer, J. W.; Hawker, C. J. *Angew. Chem., Int. Ed.* **2013**, *52*, 6844−6848.

(12) Anastasaki, A.; Nikolaou, V.; Zhang, Q.; Burns, J.; Samanta, S. R.; Waldron, C.; Haddleton, A. J.; McHale, R.; Fox, D.; Percec, V.; Wilson, P.; Haddleton, D. M. *J. Am. Chem. Soc.* **2013**, *136*, 1141−1149.

(13) Kwak, Y.; Matyjaszewski, K. *Macromolecules* **2010**, *43*, 5180−5183.

(14) Leibfarth, F. A.; Mattson, K. M.; Fors, B. P.; Collins, H. A.; Hawker, C. J. *Angew. Chem., Int. Ed.* **2013**, *52*, 199−210.

(15) Bektas, S.; Ciftci, M.; Yagci, Y. *Macromolecules* **2013**, *46*, 6751−6757.

(16) Ciftci, M.; Tasdelen, M. A.; Li, W.; Matyjaszewski, K.; Yagci, Y. *Macromolecules* **2013**, *46*, 9537−9543.

(17) Otsu, T.; Yoshida, M.; Tazaki, T. *Makromol. Chem., Rapid Commun.* **1982**, *3*, 133−140.

(18) Yamago, S.; Nakamura, Y. *Polymer* **2013**, *54*, 981−994.

(19) Ida, S.; Terashima, T.; Ouchi, M.; Sawamoto, M. *J. Am. Chem. Soc.* **2009**, *131*, 10808−10809.

(20) Wolpers, A.; Vana, P. *Macromolecules* **2014**, *47*, 954−963.

(21) Moad, G.; Rizzardo, E.; Thang, S. H. *Acc. Chem. Res.* **2008**, *41*, 1133−1142.

(22) Boyer, C.; Bulmus, V.; Davis, T. P.; Ladmiral, V.; Liu, J.; Perrier, S. *Chem. Rev.* **2009**, *109*, 5402−5436.

(23) Keddie, D. J.; Moad, G.; Rizzardo, E.; Thang, S. H. *Macromolecules* **2012**, *45*, 5321−5342.

(24) Moad, G.; Rizzardo, E.; Thang, S. H. *Chem.—Asian J.* **2013**, *8*, 1634−1644.

(25) Liu, G.; Shi, H.; Cui, Y.; Tong, J.; Zhao, Y.; Wang, D.; Cai, Y. *Polym. Chem.* **2013**, *4*, 1176−1182.

(26) Koumura, K.; Satoh, K.; Kamigaito, M. *Polym. J.* **2009**, *41*, 595−603.

(27) Quinn, J. F.; Barner, L.; Barner-Kowollik, C.; Rizzardo, E.; Davis, T. P. *Macromolecules* **2002**, *35*, 7620−7627.

(28) Zhang, H.; Deng, J.; Lu, L.; Cai, Y. *Macromolecules* **2007**, *40*, 9252−9261.

(29) Wang, H.; Li, Q.; Dai, J.; Du, F.; Zheng, H.; Bai, R. *Macromolecules* **2013**, *46*, 2576−2582.

(30) Nguyen, J. D.; D'Amato, E. M.; Narayanam, J. M. R.; Stephenson, C. R. J. *Nat. Chem.* **2012**, *4*, 854−859.

(31) Tucker, J. W.; Stephenson, C. R. J. *J. Org. Chem.* **2012**, *77*, 1617−1622.

(32) Nguyen, J. D.; Tucker, J. W.; Konieczynska, M. D.; Stephenson, C. R. J. *J. Am. Chem. Soc.* **2011**, *133*, 4160−4163.

(33) Narayanam, J. M. R.; Stephenson, C. R. J. *Chem. Soc. Rev.* **2011**, *40*, 102−113.

(34) Wallentin, C.-J.; Nguyen, J. D.; Finkbeiner, P.; Stephenson, C. R. J. *J. Am. Chem. Soc.* **2012**, *134*, 8875−8884.

(35) Lu, Z.; Yoon, T. P. *Angew. Chem., Int. Ed.* **2012**, *51*, 10329−10332.

(36) Lu, Z.; Shen, M.; Yoon, T. P. *J. Am. Chem. Soc.* **2011**, *133*, 1162−1164.

(37) Prier, C. K.; Rankic, D. A.; MacMillan, D. W. C. *Chem. Rev.* **2013**, *113*, 5322−5363.

(38) Nicewicz, D. A.; MacMillan, D. W. C. *Science* **2008**, *322*, 77−80.

(39) Flamigni, L.; Barbieri, A.; Sabatini, C.; Ventura, B.; Barigelletti, F. In *Photochemistry and Photophysics of Coordination Compounds II*; Balzani, V., Campagna, S., Eds.; Springer: Berlin, Heidelberg, 2007; Vol. *281*, pp 143−203.

(40) Alberti, A.; Benaglia, M.; Guerra, M.; Gulea, M.; Hapiot, P.; Laus, M.; Macciantelli, D.; Masson, S.; Postma, A.; Sparnacci, K. *Macromolecules* **2005**, *38*, 7610−7618.

(41) Moses, P. R.; Chambers, J. Q.; Sutherland, J. O.; Williams, D. R. *J. Electrochem. Soc.* **1975**, *122*, 608−615.

(42) Percec, V.; Guliashvili, T.; Popov, A. V.; Ramirez-Castillo, E. *J. Polym. Sci., Part A: Polym. Chem.* **2005**, *43*, 1935−1947.

(43) Rizzardo, E.; Chen, M.; Chong, B.; Moad, G.; Skidmore, M.; Thang, S. H. *Macromol. Symp.* **2007**, *248*, 104−116.

(44) Li, C.; Benicewicz, B. C. *J. Polym. Sci., Part A: Polym. Chem.* **2005**, *43*, 1535−1543.

(45) Perrier, S.; Barner-Kowollik, C.; Quinn, J. F.; Vana, P.; Davis, T. P. *Macromolecules* **2002**, *35*, 8300−8306.

(46) Vana, P.; Davis, T. P.; Barner-Kowollik, C. *Macromol. Theory Simul.* **2002**, *11*, 823−835.

(47) Goto, A.; Fukuda, T. *Prog. Polym. Sci.* **2004**, *29*, 329−385.

(48) Tsarevsky, N. V.; Matyjaszewski, K. *Chem. Rev.* **2007**, *107*, 2270−2299.

(49) Matyjaszewski, K. *Macromolecules* **2012**, *45*, 4015−4039.

(50) Braunecker, W. A.; Matyjaszewski, K. *Prog. Polym. Sci.* **2007**, *32*, 93−146.

(51) Lligadas, G.; Rosen, B. M.; Monteiro, M. J.; Percec, V. *Macromolecules* **2008**, *41*, 8360−8364.

(52) Percec, V.; Guliashvili, T.; Ladislaw, J. S.; Wistrand, A.; Stjerndahl, A.; Sienkowska, M. J.; Monteiro, M. J.; Sahoo, S. *J. Am. Chem. Soc.* **2006**, *128*, 14156−14165.

(53) Matyjaszewski, K.; Jakubowski, W.; Min, K.; Tang, W.; Huang, J.; Braunecker, W. A.; Tsarevsky, N. V. *Proc. Natl. Acad. Sci. U.S.A.* **2006**, *103*, 15309−15314.

(54) Jakubowski, W.; Matyjaszewski, K. *Angew. Chem., Int. Ed.* **2006**, *45*, 4482−4486.

(55) Elsen, A. M.; Burdyńska, J.; Park, S.; Matyjaszewski, K. *ACS Macro Lett.* **2013**, *2*, 822−825.

(56) Li, H.; Li, M.; Yu, X.; Bapat, A. P.; Sumerlin, B. S. *Polym. Chem.* **2011**, *2*, 1531−1535.
(57) Moad, G.; Chong, Y. K.; Mulder, R.; Rizzardo, E.; Thang San, H. *Controlled/Living Radical Polymerization: Progress in RAFT, DT, NMP & OMRP*; American Chemical Society: Dallas, TX, 2009; Vol. *1024*, pp 3−18.
(58) Barner-Kowollik, C. *Handbook of RAFT Polymerization*; Wiley-VCH Verlag GmbH & Co. KGaA: Weinheim, Germany, 2008; pp 1−4.
(59) Moad, G.; Barner-Kowollik, C. *Handbook of RAFT Polymerization*; Wiley-VCH Verlag GmbH & Co. KGaA: Weinheim, Germany, 2008; pp 51−104.
(60) Lowe, A. B.; McCormick, C. L. *Handbook of RAFT Polymerization*; Wiley-VCH Verlag GmbH & Co. KGaA: Weinheim, Germany, 2008; pp 235−284.
(61) Skrabania, K.; Miasnikova, A.; Bivigou-Koumba, A. M.; Zehm, D.; Laschewsky, A. *Polym. Chem.* **2011**, *2*, 2074−2083.
(62) Kwiatkowski, P.; Jurczak, J.; Pietrasik, J.; Jakubowski, W.; Mueller, L.; Matyjaszewski, K. *Macromolecules* **2008**, *41*, 1067−1069.
(63) Xu, J.; Tao, L.; Boyer, C.; Lowe, A. B.; Davis, T. P. *Macromolecules* **2009**, *43*, 20−24.
(64) Samanta, S. R.; Levere, M. E.; Percec, V. *Polym. Chem.* **2013**, *4*, 3212−3224.
(65) Lessard, B.; Tervo, C.; Marić, M. *Macromol. React. Eng.* **2009**, *3*, 245−256.
(66) Anastasaki, A.; Waldron, C.; Wilson, P.; Boyer, C.; Zetterlund, P. B.; Whittaker, M. R.; Haddleton, D. *ACS Macro Lett.* **2013**, *2*, 896−900.
(67) Gody, G.; Maschmeyer, T.; Zetterlund, P. B.; Perrier, S. *Nat. Commun.* **2013**, *4*.
(68) Soeriyadi, A. H.; Boyer, C.; Nyström, F.; Zetterlund, P. B.; Whittaker, M. R. *J. Am. Chem. Soc.* **2011**, *133*, 11128−11131.
(69) Boyer, C.; Soeriyadi, A. H.; Zetterlund, P. B.; Whittaker, M. R. *Macromolecules* **2011**, *44*, 8028−8033.
(70) Hawker, C. J.; Bosman, A. W.; Harth, E. *Chem. Rev.* **2001**, *101*, 3661−3688.
(71) Pintauer, T.; Matyjaszewski, K. *Chem. Soc. Rev.* **2008**, *37*, 1087−1097.
(72) Min, K.; Jakubowski, W.; Matyjaszewski, K. *Macromol. Rapid Commun.* **2006**, *27*, 594−598.
(73) Matyjaszewski, K.; Dong, H.; Jakubowski, W.; Pietrasik, J.; Kusumo, A. *Langmuir* **2007**, *23*, 4528−4531.
(74) Wang, G.; Lu, M.; Wu, H. *Polym. Bull.* **2012**, *69*, 417−427.
(75) Fleischmann, S.; Rosen, B. M.; Percec, V. *J. Polym. Sci., Part A: Polym. Chem.* **2010**, *48*, 1190−1196.
(76) Visnevskij, C.; Makuska, R. *Macromolecules* **2013**, *46*, 4764−4771.
(77) McMahon, J. J.; Barry, M.; Breen, K. J.; Radziwon, A. K.; Brooks, L. D.; Blair, M. R. *J. Phys. Chem. C* **2008**, *112*, 1158−1166.
(78) Zhu, S.; Das, A.; Bui, L.; Zhou, H.; Curran, D. P.; Rueping, M. *J. Am. Chem. Soc.* **2013**, *135*, 1823−1829.